Compositional and isotopic changes in expelled and residual gases during anhydrous closed system pyrolysis of hydrogen-rich Eocene subbituminous coal

Koji U. Takahashi[1], Noriyuki Suzuki[1, 2,*], Hiroyuki Saito[2]

* Corresponding author

1: Department of Natural History Sciences, Faculty of Science, Hokkaido University, N10W8, Kita-ku, Sapporo 060-0810, Japan

2: Research Division of JAPEX Earth Energy Frontier, Creative Research Institution (CRIS), Hokkaido University, N21W10, Kita-ku, Sapporo 001-0021, Japan

Abstract

Gases generated by laboratory anhydrous closed-system pyrolysis of hydrogen-rich Eocene Yubari subbituminous coal were distinguished as expelled gas, desorbed gas, residual free gas, and residual adsorbed gas, and the compositional and isotopic changes in these gases during laboratory maturation were investigated. The relative abundances of methane and H_2 in the expelled gas were higher than those in the residual free and adsorbed gases, showing compositional fractionation during gas expulsion from the coal fragments. The $\delta^{13}C$ and $\delta^{2}H$ values of ethane, propane, and CO_2 in all the gas fractions were nearly the same. However, the $\delta^{13}C$ and $\delta^{2}H$ values of methane in the residual free gas were significantly higher than those of methane in the expelled and desorbed gases, demonstrating a large isotopic fractionation associated with the expulsion of methane from the coal fragments. The carbon and hydrogen isotopic fractionations of ethane, propane, and CO_2 during their expulsion were almost negligible.

The evolution paths of the differential $\delta^{13}C$ values of hydrocarbon gases generated from hydrogen-rich Eocene Yubari coal during laboratory maturation were rather close to those of hydrocarbon gases from Type II kerogen in the early stage of maturation ($VR_r\% < 1.2$), but these shifted closer to those of hydrocarbon gases from Type III kerogen in the higher maturation stage ($VR_r\% > 1.6$). The similar $\delta^{13}C$ values of hydrocarbon gases from Eocene Yubari coal and Type II kerogen are partly due to the abundant and ^{13}C depleted aliphatic structures in the Eocene Yubari coal. The $\delta^{2}H$ of methane in expelled gas from Yubari coal also increased systematically with laboratory maturation, although it can be influenced by various factors. Estimation of the maturity level and type of source organic matter of thermogenic methane based on isotopic composition requires caution, especially in Cenozoic sedimentary basins.

1. Introduction

The enrichment of ^{13}C in thermogenic hydrocarbon gases with increasing maturation has been well studied in the laboratory and applied to evaluation of the maturity level of natural gas (e.g., Clayton, 1991; Berner et al., 1992, 1995; Andresen et al., 1995; Berner and Faber, 1996; Cramer et al., 1998; Burnham and Braun, 1998). The maturity level of natural gas provides clues for understanding natural gas behavior in a sedimentary basin because the maturity level is, in many cases, related to the timing of gas expulsion from the source rocks. The burial depth and temperature of the source rocks at the time of gas expulsion in a deep sedimentary basin are often recorded in natural gas by its maturity level. Stable carbon and hydrogen isotopic compositions of gaseous hydrocarbons are one of only a few indicators for evaluating the maturity level of natural gas. However, the isotopic composition of gaseous hydrocarbons is related not only to the maturity level but also to the type of source organic matter, biodegradation after accumulation, gas mixing, and possible isotopic fractionation during expulsion and migration, as has been discussed in many reports (e.g., Fuex, 1980; Berner et al., 1995; Prinzhofer and Huc, 1995; Prinzhofer and Pernaton, 1997; Kinnaman et al., 2007; Dai et al., 2012).

In the present study, we performed laboratory anhydrous pyrolysis to understand the compositional and isotopic changes in gases generated from Eocene subbituminous coal by artificial maturation. The carbon and hydrogen isotopic changes in gaseous hydrocarbons from Type III kerogen that occur with maturation have been investigated extensively (e.g., Berner et al., 1995; Duan et al., 2012). However, most of these studies utilized older pre-Cenozoic coals as Type III kerogen. Cenozoic coals are generally hydrogen rich compared with pre-Cenozoic coals such as those of the Carboniferous (e.g., Aihara, 1979**;** Takahashi and Aihara, 1989; Killops et al., 1994). Oil and gas fields distributed in Southeast Asia are frequently associated with Cenozoic coal fields, where coal and coaly strata are important source rocks of oil and gas (Hoffmann et al., 1984; Waseda and Nishita, 1998).

Understanding the isotopic evolution with maturation of gases from hydrogen-rich Eocene coal is one of the important objectives of the present study.

Knowledge of the compositional and isotopic differences among gases expelled from coal and retained in coal is crucial for understanding the migration and expulsion of hydrocarbon gases in coal seams and sedimentary basins. Gases associated with coal beds have been classified as desorbed, lost, and residual gases from the viewpoint of coalbed-gas resources (Bertrard et al., 1970). Desorbed gas is gas desorbed from a coal sample that was sealed in a sample container immediately after drilling and sampling. Gas desorbed from coal after drilling but before sealing in a container is called lost gas. At the time when desorbed gas measurement is discontinued, the coal sample still contains a significant amount of gas, which is called residual gas. Residual gas is present as free gas or adsorbed gas in micropore and macropore spaces within the coal matrix (Qian et al., 1996; Bustin, 1997; Strąpoć et al., 2006). Geochemical information about the isotopic and compositional changes with increasing maturation of expelled and residual gases helps us understand the behavior of coal-derived gases in a sedimentary basin. However, compared with studies of expelled gas, few studies of residual gas in coal are available.

In the present study, gases generated by laboratory anhydrous pyrolysis of Eocene subbituminous coal fragments were distinguished as (1) expelled gas, i.e., free gas expelled from coal fragments during the pyrolysis experiment; (2) desorbed gas, i.e., gas released from coal fragments at room temperature; (3) residual free gas, i.e., free gas obtained by pulverization of coal fragments; and (4) residual adsorbed gas, i.e., gas obtained from pulverized coal powder by warming it at 100ºC. The distributions and stable carbon and hydrogen isotopic compositions of CH_4, C_2H_6, C_3H_8, and CO_2 in each gas fraction were determined to investigate the isotopic evolution and isotopic and compositional fractionation of gases during thermal maturation of Eocene subbituminous coal.

2. Materials and Methods

2.1. Samples

Eocene coal-bearing strata are distributed widely from north to south in the Ishikari sedimentary basin in central Hokkaido. The Middle to Late Eocene Ishikari Group comprises the major stratigraphic sequence in the Ishikari basin. The Ishikari Group consists mainly of nonmarine to littoral sedimentary rocks with abundant coal seams, which have been exploited as the Ishikari Coal Field since the late 19th century. The Ishikari Group is divided into nine lithostratigraphic formations (Imai, 1924). The coal samples were taken from outcrops of the Middle Eocene Yubari Formation exposed at Yubari, central Hokkaido. The Yubari Formation, one of nine formations of the Ishikari Group, is composed of alternating beds of sandstone, mudstone, and coal seams deposited in fluvial and floodplain to estuarine environments (Takano and Waseda, 2003).

Before the pyrolysis experiments, the vitrinite reflectance and the organic carbon, hydrogen, total nitrogen, and total sulfur contents of the coal samples were analyzed (Table 1). The Eocene subbituminous coal is composed mainly of vitrinite, with a little degradinite (detrovitrinite), macerals. Vitrinite reflectance (VR_r) and other maturity parameters of the coal seams in the Ishikari Group show comparatively immature levels prior to the main stages of oil generation: VR_r = 0.44–0.58%, *n*-alkane CPI (C_{24} to C_{34}) = 1.3–2.3, and 20S/(20S+20R) of C_{29} regular sterane = 0.18–0.38 (Amenomori et al., 1999).

2.2. Pyrolysis of coal

Anhydrous pyrolysis experiments were conducted in a 30-mL reactor made of stainless steel 316 (Nitto Koatsu Co.). The original Yubari coal was dried at room temperature and crushed to fragments of 5–7 mm. In each experiment, a sample of about

5.0 g of coal fragments was placed in the reactor. The reactor was then evacuated for several minutes and subsequently purged with He for 5 min. The reactor was then heated rapidly to pyrolysis temperature (325–390ºC) and held isothermal for 24–168 h in a GC-14A oven (Shimadzu Co.). Higher pyrolysis temperature and shorter reaction time in artificial maturation of a coal are kinetically comparable to low temperature and long-term heating in sedimentary basins. The oven was cooled to ambient temperature before gas sampling. The pyrolysis gas expelled from the coal fragments was collected using a 1.0-L aluminum bag (GL Science Co.), and the total volume of expelled gas was measured at room temperature using a 100-mL gastight syringe (GL Science Co.). The expelled gas transfer from the reactor to the aluminum bag was completed apparently within 30 sec. The gas sampling was continued for about 5 min to reduce the isotopic fractionation during gas sampling. Void volume of reactor and tubing was calculated to be 28 mL, which was added to the total expelled gas. Gases sampled with a gastight syringe from the sampling port of the aluminum bag were analyzed as expelled gas. Desorbed gas from pyrolyzed coal fragments was obtained as follows. Pyrolyzed coal fragments were immediately placed in a 35-mL glass bottle, and the bottle was sealed with an aluminum cap with a butyl-rubber septum after purging with He for 3 min. Gases in the sealed glass bottle, which was held at room temperature for 1 week, were analyzed as desorbed gas from the pyrolyzed coal fragments.

The residual gas in pyrolyzed coal fragments can be classified as residual free gas or gas adsorbed on the coal matrix. Gas released from coal fragments during pulverization was defined as residual free gas. Pulverization of coal fragments was conducted using a P-6 planetary ball mill and a stainless-steel mill pot with needle valves and a sampling port (Fritsch Co.). The inner volume of the mill pot was 101 cm^3. Coal fragments in the size range of ca. 5–7 mm were pulverized in the stainless-steel mill pot under helium

atmosphere at a spinning rate of 300 rpm for 7 h. The temperature increase at the surface of the stainless-steel mill pot just after the pulverization was less than 3ºC at most. The grain size of the coal powder after pulverization by the ball mill was measured by a laser diffraction-scattering method using a Horiba LA-920 grain-size analyzer and determined to generally be in the range of 1–7 μm. Gas sampled with a gastight syringe directly from the sampling port of the mill pot was analyzed as residual free gas. Pulverized coal powder was transferred from the stainless steel mill pot to a 35-mL glass bottle immediately. The glass bottle was purged with He for 3 min and then sealed with an aluminum cap with a butyl-rubber septum. Gas released from the pulverized coal powder in the sealed glass bottle by warming at 100ºC for 6 h was analyzed as residual adsorbed gas.

2.3. Gas analysis

The compositions of the expelled gas, desorbed gas, and residual gas in the coal fragments were measured by gas chromatography (GC) using an Agilent 7890A equipped with a pulsed discharge helium ionization detector (PDHID) and a micropacked column containing ShinCarbon-ST 80/100 (2.0 m × 1.0 mm i.d., Shinwa Co.). The oven temperature for GC was initially programmed at 40ºC for 3 min, increasing to 300ºC at 15ºC/min, and then held at 300ºC for 15 min. Ultra-high purity He was used as the carrier gas. A constant amount of gas was introduced into the GC column using a 10- or 50-μL sampling loop. Identification of compounds was done by comparing the retention times with those of reference standards in gas mixture containing CH_4, C_2H_4, C_2H_6, C_3H_6, C_3H_8, *i*-C_4H_{10}, *n*-C_4H_{10}, H_2, CO, and CO_2. The detailed analytical method and method for identification of the gases are described in Saito et al. (2012).

2.4. Isotope analysis

Stable carbon isotopic analysis was performed by GC–combustion–isotope ratio mass spectrometry (GC-C-IRMS, Agilent 6890A GC and Finnigan MAT 252) using the same micropacked column (ShinCarbon-ST 80/100, 2.0 m x 1.0 mm i.d., Shinwa Co.) and He as the carrier gas. The GC oven temperature was programmed to 40ºC for 3 min, then to 300ºC at 15ºC/min, and finally held at 300ºC for 20 min. The combustion was performed in a micro-volume ceramic tube with CuO, NiO, and Pt wires at 900ºC. Stable hydrogen isotopic composition was measured using GC–high-temperature conversion–isotope ratio mass spectrometry (GC-HTC-IRMS, Finnigan Delta V Advantage) using the same micropacked column and He as the carrier gas. The oven temperature program was the same as that for GC-C-IRMS. The thermal conversion furnace between the GC and IRMS was maintained at 1450ºC. Stable carbon and hydrogen isotope data are reported as $\delta^{13}C$ and $\delta^{2}H$ values relative to the VPDB and VSMOW scales, respectively, according to Coplen (2011). The $\delta^{13}C$ and $\delta^{2}H$ values were determined based on a single-point calibration by comparison with the MZ3-01 CH_4 standard ($\delta^{13}C$ of -31.1‰; SI Science Co.) and the Indiana CH_4 #1 standard ($\delta^{13}C$ of -38.25‰ and $\delta^{2}H$ of -160.8‰; Indiana Univ.), respectively. The $\delta^{13}C$ value of MZ3-01 CH_4 standard has been calibrated against NBS 19. The $\delta^{13}C$ and $\delta^{2}H$ values of Indiana CH_4 #1 standard are normalized to NBS 19/L-SVEC and SLAP, respectively. The H_3^+ factor of the mass spectrometer was determined once each day using external reference gas injections and was consistently <10 ppm. The selected gas samples were measured for $\delta^{13}C$ and $\delta^{2}H$ values repeatedly 4 to 5 times. The result showed the analytical precisions of $\delta^{13}C$ and $\delta^{2}H$ values were ±0.46‰ and ±7‰ at most, respectively.

2.5. Measurement of vitrinite reflectance

Vitrinite reflectance (VR_r) was measured using a reflecting microscope (ECLIPSE

LV100ND, Nikon, Ltd.) equipped with a stabilized halogen light source and photonic multichannel analyzer (PMA12, Hamamatsu Photonics Co.). The VR_r value was measured for a spot diameter of 20 μm at a wavelength of 542.8 nm by comparison with the standard values of polished glasses with VR_r values of 0.55, 0.79, 1.08, and 1.53%, respectively. The mean VR_r value of a coal sample was determined based on a VR_r dataset obtained from more than 50 spots. The error of VR_r measurement was within ±0.03% in the VR_r range of 0.3–2.0%.

3. Result and discussion

3.1. Composition of expelled and residual gases

The maturity levels of Eocene Hokkaido coals exposed in the outcrops are generally in the limited range of VR_r = 0.5–0.9% (Amenomori et al., 1999; Suzuki and Fujii, 1999). Artificial maturation of the Eocene Yubari coal was therefore performed to understand the compositional and isotopic changes in expelled, desorbed, and residual gases with increasing maturation. The VR_r value of the Eocene Yubari coal used in the present study was measured at 0.46%, a maturity level of subbituminous coal. The VR_r values of artificially matured coals (AMCs) #1 through #5 were in the range of 0.53–1.46% (Table 2). The VR_r values of AMC #6 and AMC #7 could not be determined because substantial bituminous organic matter generated during the heating experiment prevented correct measurement of VR_r due to suppression of VR_r. According to Huang (1996), VR_r values of AMC #6 and AMC #7 were estimated to be 1.7 and 1.8%, respectively, based on heating temperature and heating time.

Typical PDHID gas chromatograms of expelled, desorbed, residual free, and residual adsorbed gases are shown in Fig. 1. O_2 and N_2 are contaminants from the air. The expelled gas was generally characterized by higher relative abundances of CH_4 (C_1), C_2H_6

(C_2), and H_2. The gas composition of the desorbed gas was similar to that of the expelled gas, except for comparatively low abundances of H_2, C_3H_8 (C_3), and C_4H_{10} (C_4) (Fig. 1 and Table 2). The residual free gas obtained after pulverization of the coal fragments showed lower relative abundance of C_1 compared with the expelled gas. The hydrogen in the residual free gas could have been derived partly from H_2 generated by stainless steel metal–metal friction. The residual adsorbed gas was characterized by a very low concentration of C_1 and higher relative abundances of CO_2, C_3, and C_4 (Fig. 1). The $C_1/(C_2 + C_3)$ mole ratios of the expelled gas and desorbed gas were generally higher than those of the residual free gas and residual adsorbed gas obtained from the same heating experiment, as shown in Fig. 2. The residual adsorbed gas showed remarkably high values for the $CO_2/(CO_2 + C_1)$ mole ratio (Fig. 2 and Table 2). The different gas compositions of the various gas fractions from the coal are attributed to the different mobilities and adsorption coefficients of the gas components in the coal matrix. Lower molecular hydrocarbon gases such as C_1 and C_2 are more mobile, as they do not have significant interaction with the coal matrix. A considerable amount of C_1 can be easily expelled outside of coal during the maturation process in the laboratory. The higher abundances of CO_2 and C_4 in the residual adsorbed gas are very consistent with their adsorptive characteristics (e.g., Mastalerz et al., 2004; Fitzgerald et al., 2006; Harpalani et al., 2006). Considering the low temperature of the sedimentary basin, significant amounts of CO_2 and C_4 are thought to be present as gases adsorbed on the coal matrix. The different gas compositions of the gas fractions show that compositional fractionation takes place in association with the expulsion and migration of natural gas in coal seams, as was suggested in previous studies (e.g., Rice, 1993; Price and Schoell, 1995; Pepper and Corvi, 1995).

3.2. Changes in gas composition with maturation

The composition of gas generated from source rocks during maturation, whether in the laboratory or in a natural setting, depends on the type of kerogen and the maturity level of the source rocks (Galimov, 1988; Schoell, 1988; Andresen et al., 1995; Clayton, 1998). The gas generated during maturation changes to dry gas in the higher stage of maturation.

The concentrations of C_1 to C_4 hydrocarbons in the expelled gas were generally the highest among those of all the gas fractions except for that of AMC#1, and these increased with increasing maturation. However, the concentrations of C_2 to C_4 hydrocarbons in the desorbed gas were variable and did not show a systematic trend with maturation, although C_1 in desorbed gas tended to increase with increasing maturation. The concentration of C_1 in the desorbed gas tended to be higher than those in the residual free and residual adsorbed gases, whereas the concentration of C_4 hydrocarbon tended to be lower than those in the residual adsorbed gas. $C_1/(C_2 + C_3)$ mole ratios (gas dryness) of the expelled, desorbed, residual free, and residual adsorbed gases tended to decrease with maturation in the initial stage of maturation (up to $VR_r = 1.0\%$) and then increase with maturation, except for the gas dryness of residual adsorbed gas, in the higher stage of maturation ($VR_r > 1.0\%$). The gas dryness in the residual adsorbed gas was generally very low and decreased with increasing maturation (Fig. 2).

The decrease in gas dryness with maturation in the initial stage was due to the generation of C_2 and C_3 hydrocarbons by the primary cracking of aliphatic structures in the coal. The subsequent increase in gas dryness was attributable to further cracking of short-chain aliphatic structures in the coal to generate C_1 at an advanced stage of maturity. The very low abundance of C_1 in the residual adsorbed gas is thought to have been due to the lower-adsorptive nature of the C_1 compared with the C_2 and C_3 hydrocarbons and selective expulsion of C_1 from the coal fragments. The relative abundance of C_1 in the residual free gas was also generally lower than those of the expelled and desorbed gases,

illustrating selective expulsion of C_1 from the coal fragments (Fig. 2).

On the other hand, all of the gas fractions contained a significant amount of unsaturated hydrocarbons, such as C_2H_4 and C_3H_6 (Fig. 1 and Table 2). Anhydrous pyrolysis of sedimentary organic matter under an inert gas atmosphere generally produces abundant unsaturated hydrocarbons (e.g., Ishiwatari and Fukushima, 1979; Lewan, 1997), suggesting a lack of H_2 for hydrogenation of unsaturated compounds. However, a significant amount of H_2 was detected in the expelled and residual free gases (Fig. 1 and Table 2). The desorbed and residual adsorbed gases contained only a small amount of H_2, demonstrating its mobility and non-adsorptive nature. The presence of abundant unsaturated hydrocarbons with sufficient H_2 could be due to the absence of a catalyst that could promote hydrogenation of the unsaturated hydrocarbons. Pyrolysis experiment of coal in the near absence of water could also be responsible for the presence of abundant unsaturated hydrocarbons as suggested by Lewan (1997).

The concentration of CO_2 in the expelled gas was the highest among those of all the gas fractions and increased with maturation. However, the relative abundance of CO_2 in the gas fractions except for residual desorbed gas fraction decreased markedly with increasing artificial maturation (Fig. 2). The CO_2 was derived mainly from oxygen-containing functional groups, such as carbonyl and carboxyl groups, in the coal matrix. The generation of CO_2 from coal mainly proceeds in the early stage of thermal alteration, resulting in a higher $CO_2/(CO_2 + CH_4)$ mole ratio of all gas fractions in the early stage of maturation.

3.3 Isotopic characteristics of expelled and residual gases

The $\delta^{13}C$ values of C_1, C_2, and C_3 ($\delta^{13}C_1$, $\delta^{13}C_2$, and $\delta^{13}C_3$) in the expelled, desorbed, and residual free gases were in the range of -42 to -26‰ (Table 2 and Fig. 3) and showed significant variation in values. These $\delta^{13}C$ values are similar to the carbon isotope ratios of

thermogenic hydrocarbon gases (e.g., Shoell, 1980; Jenden et al., 1993; Whiticar, 1996; Pohlman et al., 2005). The relationship $\delta^{13}C_1 < \delta^{13}C_2 < \delta^{13}C_3$ was observed generally in all the gas fractions, although the $\delta^{13}C_1$, $\delta^{13}C_2$, and $\delta^{13}C_3$ in the residual free gas were in a relatively limited range of -33 to -26‰ compared with those in the other gas fractions. The $\delta^{13}C$ values of CO_2 in the expelled, adsorbed, and residual free gases were in the relatively limited range of -28 to -20‰, which is higher than those of the hydrocarbon gases in the same gas fraction. The δ^2H values of C_1 (δ^2H_{C1}) in the residual free gas were in the range of -240 to -180‰, which is obviously higher than the δ^2H_{C1} (-350 to -250‰) in the expelled and desorbed gases. The δ^2H values of C_2H_6 and C_3H_8 (δ^2H_{C2} and δ^2H_{C3}) in the expelled, adsorbed, and residual free gases were in the range of -300 to -200‰ (Table 2 and Fig. 4).

The $\delta^{13}C_1$ values of the residual free gas in the coal fragments were 3–10‰ higher than those in the expelled gas (Fig. 3). However, all the $\delta^{13}C_2$ and $\delta^{13}C_3$ values in the expelled, desorbed, and residual free gases were nearly the same. Similar isotopic characteristics were obtained for δ^2H_{C1}, δ^2H_{C2}, and δ^2H_{C3}. The δ^2H_{C1} in the residual free gas was 20–120‰ higher than those in the expelled gas, and the δ^2H_{C2} and δ^2H_{C3} in the expelled, desorbed, and residual gases were almost the same (Fig. 4). These isotopic characteristics suggest that large isotopic fractionation took place in association with the expulsion of CH_4 from the coal fragments. Apart from the effects of gas source and generation mechanism, compositional and isotopic fractionations during gas migration have been invoked recurrently to explain and interpret natural gas systems. Some studies have ascribed large changes in $\delta^{13}C_1$ values (>5‰) to diffusive migration effects in coal (Prinzhofer and Huc, 1995; Prinzhofer and Pernaton, 1997). Zhang and Krooss (2001) suggested that the diffusive isotope fractionation of C_1 in shale depends on TOC content. A large isotopic fractionation would be expected to occur during diffusive migration of C_1 in coal matrix and coal seams in a sedimentary basin because coal generally has abundant organic matter that interacts

with migrating gaseous hydrocarbons. Gaseous components generated in coal can have much chance to interact with organic matrix in the coal seams before their expulsion. Carbon and hydrogen isotopic fractionation during migration of CH_4 in coal seams could be one of the important processes controlling the isotopic composition of CH_4 in expelled gas. The present study, however, showed that carbon and hydrogen isotopic fractionations in C_2, C_3, and CO_2 during their migration and expulsion are almost negligible.

3.4 Changes in isotopic composition with maturation

The $\delta^{13}C$ and $\delta^{2}H$ values of hydrocarbon gases and CO_2 in the expelled gas increased with increasing artificial maturation, although the $\delta^{13}C_1$ value tended to decrease with maturation in the early stage of artificial maturation ($VR_r < 1.3\%$) (Fig. 3). The $\delta^{13}C$ value of CH_4 generated in the initial stage of pyrolysis experiments is often relatively large (Berner et al., 1995; Cramer et al., 1998; Tang et al., 2000; Gaschnitz et al., 2001) (Fig. 3). Berner et al. (1995) observed a similar change in $\delta^{13}C_1$ in their pyrolysis experiments ($VR_r = 1.59\%$) and interpreted the change in terms of the mixing of gases generated from two different groups of reactions. The first reaction group may have produced methane rich in ^{13}C at lower temperatures that was continuously overwhelmed by methane poor in ^{13}C derived from a second group of reactions at higher temperatures. According to Chung and Sackett (1980) and Smith et al. (1985), the earliest methane can be generated from a pool of isotopically heavy methyl groups bound by relatively labile C–O or C–S linkages. The $\delta^{13}C_1$ in the expelled gas then becomes lighter at moderate temperature and subsequently becomes heavier again with increasing temperature in the higher maturation stage ($VR_r > 1.3\%$). Tang et al. (1996) also interpreted that the overall change in $\delta^{13}C_1$ in pyrolysis experiments can be explained by hypothesizing two or more precursors for CH_4 generation with different isotopic compositions. The initial trend of decreasing $\delta^{13}C_1$ in Fig. 3, therefore, could be

explained by mixing with CH_4 generated from isotopically lighter and more tightly bound precursors (Tang and Jenden, 1998). In the higher maturation stage (VR_r > 1.3%), $\delta^{13}C_1$ finally increases with increasing maturation (Fig. 3). Enrichment of ^{13}C in natural gas with increasing temperature has been well documented (Clayton, 1991; Andresen et al., 1995; Schenk et al., 1997; Cramer et al., 1998; Burnham and Braun, 1998). The increase in $\delta^{13}C_1$ in the higher maturation stage is due to the mixing of CH_4 generated from isotopically heavier and more tightly bound aliphatic structures in kerogen and bitumen. The same explanation can be applied to the increases in the δ^2H values of hydrocarbon gases with maturation in the expelled and desorbed gases (Fig. 4). However, the $\delta^{13}C$ and δ^2H values of CH_4 in the residual free gas at the highest maturity level (VR_r = ca. 1.8%) decreased significantly (Figs. 3 and 4). The coal fragments (AMC #7) after the pyrolysis experiment at 390ºC for 168 h were sticky and contained much bituminous organic matter that prevented VR_r measurement, as described previously. The comparatively similar values of $\delta^{13}C_1$ and δ^2H_{C1} in both the expelled and residual free gases (Figs. 3 and 4) suggest that high amounts of bituminous organic matter distributed in the coal matrix reduced the surface effect on the isotopic fractionation between coal and C_1. Hydrocarbon gases are soluble in liquid hydrocarbons especially under high pressure. The exsolution of dissolved methane from bitumen could be another possible reason for the similar values of $\delta^{13}C_1$ and δ^2H_{C1} in both the expelled and residual free gases

The $\delta^{13}C$ of CO_2 in the expelled gas increased slightly from -25 to -23‰ with maturation, but that in the desorbed and residual free gases was quite variable. The CO_2 concentrations of the desorbed and residual free gases were also variable and did not show any systematic changes with maturation. The uncertainty in the measurements of the $\delta^{13}C$ value and concentration of CO_2 is thought to be due to the adsorptive characteristics of CO_2, as the interaction between CO_2 and the surface of the coal powder during coal pulverization

and preservation in the glass vial prevents correct measurement of the $\delta^{13}C$ value and CO_2 concentration in the desorbed and residual free gases. This effect is minor in the case of CO_2 in the expelled gas, which has very high concentration compared with that in the desorbed and residual free gases. The CO_2 concentration in the expelled gas increased systematically with maturation (Table 2), resulting in an increase in the $\delta^{13}C$ value of CO_2 with maturation. The increasing trend of $\delta^{13}C$ of CO_2 in the expelled gas can be explained by mixing with CO_2 generated from isotopically heavier and more tightly bound precursors.

3.5 Isotopic evolution of expelled gas from hydrogen-rich Eocene coal

The $\delta^{13}C$ values of CH_4, C_2H_6, and C_3H_8 generated from kerogen during open-system pyrolysis increase progressively with increasing maturity (Andresen et al., 1993; Berner and Faber, 1996). The $\delta^{13}C$ values of CH_4, C_2H_6, and C_3H_8 in the present study were obtained from the cumulative gas generated during closed-system pyrolysis. It is therefore difficult to directly compare the $\delta^{13}C$ dataset of the present study with those from open-system pyrolysis. In the present study, the differential values of $\delta^{13}C_1$, $\delta^{13}C_2$, and $\delta^{13}C_3$ were calculated based on the extrapolated cumulative changes in $\delta^{13}C$ values and volumes of C_1, C_2, and C_3 generated from Eocene Yubari coal by closed-system pyrolysis. The differential values of $\delta^{13}C_1$, $\delta^{13}C_2$, and $\delta^{13}C_3$ were calculated for every interval of 0.2% VR_r. The results of the calculations for the differential variations in $\delta^{13}C_1$, $\delta^{13}C_2$, and $\delta^{13}C_3$ values with increasing VR_r are plotted in Fig. 5. Following Berner and Faber (1996), the progressive increases in $\delta^{13}C_1$, $\delta^{13}C_2$, and $\delta^{13}C_3$ for gases from Type II and Type III kerogens were calculated and also plotted in Fig. 5, assuming that the $\delta^{13}C$ values of the original Type II and Type III kerogens were -22.3‰ and -25.8‰, respectively (Waseda and Nishita, 1998; Waseda et al., 2002). The differential variation in $\delta^{13}C$ in closed-system pyrolysis is not the same as that in open-system pyrolysis because the thermal conversion from C_2 and C_3 to C_1

in the cumulative gas during closed-system pyrolysis increases the total amount of C_1 compared with the case of open-system pyrolysis. A detailed comparison between open-system and closed-system pyrolysis will be discussed in a future manuscript.

The evolution paths of $\delta^{13}C_1$ vs. $\delta^{13}C_2$ and $\delta^{13}C_2$ vs. $\delta^{13}C_3$ of Eocene Yubari coal were drawn nearly between the evolution paths of gases from Type II kerogen and Type III kerogen based on Berner and Faber (1996) (Fig. 5). The evolution path of $\delta^{13}C_1$ vs. $\delta^{13}C_2$ in hydrocarbon gas from Eocene Yubari coal in the early stage of maturation ($VR_r < 1.2\%$) is rather close to that of Type II kerogen (Fig. 5). At the higher maturity level ($VR_r > 1.6\%$), the $\delta^{13}C_1$ vs. $\delta^{13}C_2$ evolution path of Yubari coal shifts closer to that of the Type III kerogen drawn based on Berner and Faber (1996) (Fig. 5). A similar relationship was observed in the evolution path of $\delta^{13}C_2$ vs. $\delta^{13}C_3$. The $\delta^{13}C_2$ vs. $\delta^{13}C_3$ evolution path of Yubari coal is close to that of Type II kerogen at the lower maturity level ($VR_r < 1.2\%$), but it shifts close to that of Type III kerogen at the higher maturity level ($VR_r > 1.6\%$), as shown in Fig. 5.

The $\delta^{13}C$ value of thermogenic hydrocarbons is related not only to the maturity level but also to the $\delta^{13}C$ value of the source organic matter and the kerogen type. Gaseous C_1 to C_3 hydrocarbons from Type III kerogen are derived mainly from short-chain aliphatic structures bound to aromatic rings, whereas those from Type II kerogen significantly contain hydrocarbons from long polymethylene chains. The $\delta^{13}C$ value of aliphatic compounds is generally lower than that of aromatic compounds (e.g., Stahl, 1977; Robinson et al., 1991; Waseda and Nishita, 1998), resulting in the lower $\delta^{13}C$ values of gaseous hydrocarbons from Type II kerogen compared with those from Type III kerogen. The $\delta^{13}C_1$ in natural gas derived from marine-source organic matter is generally lower than that from terrestrial-source organic matter (Berner et al., 1995; Sakata et al., 1997; Dai et al., 2012). Cenozoic coals and coaly sediments have the potential to generate oil, which is related to the abundant aliphatic structures in Cenozoic coals compared with older Carboniferous coals

(MacGregor, 1994; Petersen and Nytoft, 2006; Petersen et al., 2009). Cenozoic coal strata, therefore, are important source rocks for oil (e.g., the Niger delta in Nigeria, Mahakam delta in Indonesia, Taranaki basin in New Zealand, and Ishikari basin in Japan). The Eocene coals in the Ishikari basin are hydrogen rich (Aihara, 1979; Takahashi and Aihara, 1989; Suzuki and Fujii, 1999), are characterized by a relatively high hydrogen index (HI = 228 to 476 mg HC/g TOC) (Amenomori et al., 1999), and are important source rocks of the Yufutsu oil and gas fields, Japan (Waseda and Nishita, 1998; Yessalina et al., 2006). The hydrocarbon generation potential is generally linked to the hydrogen content of coal. Perhydrous coals rich in hydrogen are known to generate oil (Wilkins and George, 2002). The Eocene Yubari coal of the present study is also characterized by relatively high atomic H/C, as shown in Table 1. The similarity between the $\delta^{13}C$ evolution paths of gases from Eocene Yubari coal and from Type II kerogen in the early stage of maturation (VR_r < 1.2%) could be partly attributable to the abundant and isotopically lighter aliphatic structures in Yubari coal. The Eocene coals generally contain a significant amount of organic matter derived from angiosperms. Murray et al. (1998) suggested that typical $\delta^{13}C$ values for gymnosperm and angiosperm resins are -22.8 and -26.4%, respectively. Chikaraishi et al. (2004) and Chikaraishi and Naraoka (2007) also reported that bulk $\delta^{13}C$ values of angiosperms were lighter than those of gymnosperms. The lighter $\delta^{13}C$ value of angiosperms could be another reason for the lighter $\delta^{13}C$ values of gaseous hydrocarbons generated from the Eocene Yubari coal. The $\delta^{13}C$ evolution paths of Yubari coal shift closer to those of Type III kerogen in the later stage of maturation (VR_r > 1.6%), showing that sources of gaseous hydrocarbons in the Eocene Yubari coal and in typical Type III kerogen have similar isotopic signatures after significant hydrocarbon generation. This may be due to a similarity in basic chemical structures between Eocene Yubari coal and Type III kerogen in the higher maturation stage.

The differential variation in $\delta^{2}H_{C1}$ with increasing maturation was similarly

estimated based on the cumulative changes in the δ^2H value and the CH_4 concentration of expelled gas during closed-system pyrolysis. The differential δ^2H_{C1} in the expelled gas increased systematically from -330 to -110‰ with increasing maturation from VR_r = 0.5 to 2.0% (Fig. 6). The δ^2H_{C1} vs. VR_r for Type II and Type III kerogens (Berner et al., 1995) are also plotted in Fig. 6. The evolution path of the differential δ^2H_{C1} of expelled gas from the Yubari coal is close to that of δ^2H_{C1} from Type III kerogen in the early stage of maturation (VR_r < 1.5%), but it is rather close to that of δ^2H_{C1} from Type II kerogen in the later stage of maturation (VR_r > 1.5%). This relationship is different from the relationship in $\delta^{13}C_1$ shown in Fig. 5.

The increase in the differential δ^2H_{C1} with artificial maturation can be explained by mixing with isotopically heavier CH_4 with increasing maturation, as was discussed previously. The pyrolysis experiments in the present study were performed under non-hydrous conditions. However, inorganic hydrogen from water can be added to and/or exchanged with organic hydrogen during hydrous pyrolysis (Hoering, 1984; Lewan, 1997; Schimmelmann et al., 1999, 2001). Hydrogen exchange between interstitial water and sedimentary organic matter in the early stage of diagenesis has been suggested (Lis et al., 2006; Schimmelmann et al., 2006; Kikuchi et al., 2010). Hence, the influence of water-derived hydrogen on the δ^2H of thermogenic CH_4 cannot be ignored. The δ^2H values of higher plant wax and isoprenoid compounds show significant variation in the range of -250 to -100‰ and -400 to -200‰, respectively (e.g., Chikaraishi and Naraoka, 2007; Hou et al., 2007; Li et al. 2009; Sachse et al., 2010), suggesting a wide range of initial δ^2H values of coals. The δ^2H of higher land plants is also related to the climate humidity or aridity (e.g., Tipple and Pagani, 2010; Duan et al., 2011; Yang et al., 2011). It could be difficult to evaluate source kerogen type and the maturity level of CH_4 using δ^2H_{C1}. The lower δ^2H_{C1} of Yubari coal in the early stage of maturation (VR_r < 1.5%) could be due to the

swampy and aqueous depositional environment and the warm and humid climate that existed in Eocene time as well as the anhydrous pyrolysis experiment. The $\delta^{13}C$ and $\delta^{2}H$ values of C_1 provide useful information about the type of source organic matter (Schoell, 1980, 1988). The present study, however, suggests that estimation of the origin of thermogenic C_1 based on isotopic composition requires caution, especially in Cenozoic sedimentary basins.

4. Conclusions

In the present study, gases generated by laboratory anhydrous pyrolysis of Eocene Yubari subbituminous coal were distinguished as expelled gas, desorbed gas, residual free gas, or residual adsorbed gas. The relative abundances of C_1, C_2, and H_2 in the expelled gas were generally higher than those of the residual free and adsorbed gases. The residual adsorbed gas showed a remarkably high abundance of CO_2. The different gas compositions of the various gas fractions show the compositional fractionation during expulsion from the coal fragments. The isotopic characteristics of the various gas fractions suggest that large isotopic fractionation took place in association with the expulsion of CH_4 from the coal fragments. The carbon and hydrogen isotopic fractionations that occur during migration of CH_4 in coal seams can be one of the important processes controlling the isotopic composition of CH_4 in expelled gas. The present study, however, showed that the carbon and hydrogen isotopic fractionations of C_2H_6, C_3H_8, and CO_2 during migration and expulsion are almost negligible.

The evolution paths of $\delta^{13}C$ values of hydrocarbon gases in the expelled gas from the hydrogen-rich Eocene Yubari coal were rather close to those of Type II kerogen in the early stage of maturation ($VR_r < 1.2\%$). At the higher maturity level ($VR_r > 1.6\%$), the paths shifted closer to those of Type III kerogen. The differential $\delta^{2}H_{C1}$ in the expelled gas

increased systematically during laboratory maturation. However, it might be difficult to evaluate the maturity level of CH_4 based only on the δ^2H_{C1} value, as δ^2H_{C1} can be controlled by various factors in nature.

The present study supports that carbon isotope compositions of C_1 to C_3 are useful indicators for evaluating the maturity level of natural gas. However, $\delta^{13}C$ values of C_1 to C_3 derived from coals and coaly mudstones are susceptible to the organic composition of the source material, which is also related to the evolution of higher plants. The δ^2H of C_1 can be controlled by various factors, such as the type of source higher plants, the paleohydrology, and hydrogen exchange during maturation in the sedimentary basin. The estimation of the origin of thermogenic C_1 based on isotopic composition requires caution, especially in Cenozoic sedimentary basins.

Acknowledgment

This research was supported by a Grant-in-Aid for Scientific Research (no. 21540466: N. Suzuki) from the Ministry of Education, Culture, Sports, Science and Technology (MEXT) of Japan and by a research donation from the Japan Petroleum Exploration Co., Ltd. (JAPEX). We thank Professor Y. Sampei of Shimane University for his kind help in calibrating standard glasses for vitrinite reflectance measurement and Dr. T. Irino for his help and instructions in grain-size analysis of the pulverized coal samples. Thanks are also due to Dr. A. Schimmelmann and anonymous reviewer for comments which improved the manuscript.

References

Aihara, A., 1979. Organic metamorphism and petroleum generation in upper Cretaceous and Tertiary Systems of Hokkaido, Japan. (in Japanese with English abstract). Journal of the Japanese Association for Petroleum Technology 44, 124–133.

Amenomori, G., Konishi, T., Suzuki, N., Iguchi, T., 1999. Petroleum geochemical characteristics of degradinatite-rich Eocene coals and coaly mudstones, Hokkaido, Japan. Researches in Organic Geochemistry 14, 33–41 (in Japanese with English Abstract).

Andresen, B., Barth, T., Irwin, H., 1993. Yields and carbon isotope composition of pyrolysis products from artificial maturation processes. Chemical Geology 106, 103–119.

Andresen, B., Throndsen, T., Raheim, A., Bolstad, J., 1995. A comparison of pyrolysis products with models for natural gas generation. Chemical Geology 126, 261–280.

Berner, U., Faber, E., 1996. Empirical carbon isotope/maturity relationships for gases from algal kerogens and terrigenous organic matter, based on dry, open-system pyrolysis. Organic Geochemistry 24, 947–955.

Berner, U., Faber, E., Scheeder, G., Panten, D., 1995. Primary cracking of algal and land plant kerogens: kinetic models of isotope variations in methane, ethane and propane. Chemical Geology 126, 233–245.

Berner, U., Faber, E., Stahl, W., 1992. Mathematical simulation of the carbon isotope fractionation between huminitic coal and related methane. Chemical Geology 94, 315-319.

Bertrard, D., Byuyet, B., Gunter, J., 1970. Determination of desorbed gas concentration of coal direct method. International Journal of Rock Mechanics and Mining science 7, 43–65.

Burnham, A.K., Braun, R.L., 1998. Global kinetic analysis of complex materials. Energy &

Fuels 13, 1–22.

Bustin, R.M., 1997. Importance of fabric and composition on the stress sensitivity of permeability in some coals, northerrn Sydney Basin, Australia; relevance to coalbed methane explotation. AAPG Bulletin 81, 1894–1908.

Chikaraishi, Y., Naraoka, H., 2007. δ^{13}C and δD relationships among three *n*-alkyl compound classes (*n*-alkanoic acid, *n*-alkane and *n*-alkanol) of terrestrial higher plants. Organic Geochemistry 38, 198–215.

Chikaraishi, Y., Naraoka, H., Poulson, S.R., 2004. Hydrogen and carbon isotopic fractionations of lipid biosynthesis among terrestrial (C3, C4 and CAM) and aquatic plants. Phytochemistry 65, 1369-1381.

Chung, H.M., Sackett, W.M., 1980. Carbon isotope effects during the pyrolytic formation of early methane from carbonaceous materials. In: Douglas, A.G., Maxwell, J.R. (Eds.), Advances in Organic Geochemistry 1979, Pergamon Press, 705–710.

Clayton, C., 1991. Carbon isotope fractionation during natural-gas generation from kerogen. Marine and Petroleum Geology 8, 232–240.

Clayton, J.L., 1998. Geochemistry of coalbed gas - A review. International Journal of Coal Geology 35, 159–173.

Coplen, T.B., 2011. Guidelines and recommended terms for expression of stable isotope-ratio and gas-ratio measurement results. Rapid Communications in Mass Spectrometry 25, 2538-2560.

Cramer, B., Krooss, B.M., Littke, R., 1998. Modeling isotope fractionation during primary cracking of natural gas: a reaction kinetic approach. Chemical Geology 149, 235–250.

Dai, J., Ni, Y., Zou, C., 2012. Stable carbon and hydrogen isotopes of natural gases sourced from the Xujiahe Formation in the Sichuan Basin, China. Organic Geochemistry 43, 103–111.

Duan, Y., Sun, T., Qian, Y., He, J., Zhang, X., Xu, L., Wu, B., 2012. Pyrolysis experiments of forest marsh peat samples with different maturities: An attempt to understand the isotopic fractionation of coalbed methane during staged accumulation. Fuel 94, 480–485.

Duan, Y., Wu, B., Xu, L., He, J., Sun, T., 2011. Characterisation of *n*-alkanes and their hydrogen isotopic composition in sediments feom Lake Qinghai, China. Organic Geochemistry 42, 720–726.

Fitzgerald, J.E., Robinson Jr., R.L., Gasem, K.A., 2006. Modeling high-pressure adsorption of gas mixtures on activated carbon and coal using a simplified local-density model. Langmuir 7, 9610–9618.

Fuex, A.N., 1980. Experimental evidence against an appreciable isotopic fractionation of methane during migration. In: Douglas, A.G., Maxwell, J.R. (Eds.), Advances in Organic Geochemistry 1979, Pergamon Press, 725–732.

Galimov, E.M., 1988. Sources and mechanisms of formation of gaseous hydrocarbons in sedimentary rocks. Chemical Geology 71, 77-95.

Gaschnitz, R., Krooss, B.M., Gerling, P., Faber, E., Litike, R., 2001. On-line pyrolysis-GC-IRMS: isotope fractionation of thermally generated from coals. Fuel 80, 2139–2153.

Harpalani, S., Prusty, B.K., Dutta, P., 2006. Methane/CO_2 sorption modeling for coalbed methane production and CO_2 sequestration. Energy & Fuels 20, 1591–1599.

Hoering, T.C., 1984. Thermal reaction of kerogen with added water, heavy water, and pure organic substances. Organic Geochemistry 5, 267–278.

Hoffmann, C.F., Mackenzie, A.S., Lewis, C.A., Maxwell, J.R., Oudin, J.L., Durand, B., Vamdenbroucke, M., 1984. A biological marker study of coals, shales and oils from Mahakam Delta, Kalimantan, Indonesia. Chemical Geology 42, 1–23.

Hou, J., D'Andrea, W., MacDonald, D., Huang, Y.S., 2007. Hydrogen isotopic variability in leaf waxes among terrestrial and aquatic plants around Blood Pond, Massachusetts (USA). Organic Geochemistry 38, 977–984.

Huang, W.L., 1996. Experimental study of Vitrinite maturation: effects of temperature, time, pressure, water, and hydrogen index. Organic Geochemistry 24, 233–241.

Imai, H., 1924. Stratigraphic study on the coal-bearing Tertiary (Ishikari Series) in the Ishikari Coal Field: Part 1. Journal of Geographical Society of Japan 36**,** 133–157 (in Japanese).

Ishiwatari, R., Fukushima, K., 1979. Generation of unsaturated and aromatic hydrocarbons by thermal alteration of young kerogen. Geochimica et Cosmochimica Acta 43, 1343–1349.

Jenden, P.D., Hilton, D.R., Kaplan I.R., Craig, H., 1993. Abiogenic hydrocarbons and mantle helium in oil and gas fields. U. S. Geological Survey Professional Paper 1570, 31–56.

Kikuchi, T., Suzuki, N., Saito, H., 2010. Change in hydrogen isotope composition of *n*-alkanes, pristine, phytane, and aromatic hydrocarbons in Miocene siliceous mudstones with increasing maturity. Organic Geochemistry 41, 940–946.

Killops, S.D., Woolhouse, A.D., Weston, R.J., Cook, R.A., 1994. A geochemical appraisal of oil generation in the Taranaki Basin, New Zealand. American Association of Petroleum Geologists Bulletin 78, 1560–1585.

Kinnaman, F.S., Valentine, D.L., Tyler, S.C., 2007. Carbon and hydrogen isotope fractionation associated with the aerobic microbial oxidation of methane, ethane, propane and butane. Geochimica et Cosmochimica Acta 71, 271–283.

Lewan, M.D., 1997. Experiments on the role of water in petroleum formation. Geochimica et Cosmochimica Acta 61, 3691–3723.

Li, C., Sessions, A.L., Kinnaman, F.S., Valentine, D.L., 2009. Hydrogen-isotopic variability in lipids from Santa Barbara Basin sediments. Geochimica et Cosmochimica Acta 73, 4803–4823.

Lis, G.P., Schimmelmann, A., Mastalerz, M., 2006. D/H ratios and hydrogen exchangeability of type-II kerogens with increasing thermal maturity. Organic Geochemistry 37, 342–353.

MacGregor, D.S., 1994. Coal-bearing strata as source rocks, -a grobal overview. In: Scott, A. C., Fleet, A.J. (eds), Coal and coal-bearing strata as oil-prone source rocks? Geological Society London Special Publication, 77, 107–116.

Mastalerz, M., Gluskoter, H., Rupp, J., 2004. Carbon dioxide and methane sorption in high volatile bituminous coals from Indiana, USA. International Journal of Coal Geology 60, 43–55.

Murray, A.P., Edwards, D., Hope, J.M., Boreham, C.J., Booth, W.E., Alexander, R.A., Summons, R.E., 1998. Carbon isotope biogeochemistry of plant resins and derived hydrocarbons. Organic Geochemistry 29, 1199–1214.

Pepper, A.S., Corvi, P.J., 1995. Simple kinetic models of petroleum formation, Part III: Modeling an open system. Marine and Petroleum Geology 12, 417–452.

Petersen, H.I., Nytoft, H.P., 2006. Oil generation capacity of coals as a function of coal age and aliphatic structure. Organic Geochemistry 37, 558–583.

Petersen, H.I., Lindström, S., Nytoft, H.P., Rosenberg, P., 2009. Composition, peat-forming vegetation and kerogen paraffinicity of Cenozoic coals: Relationship to variations in the petroleum generation potential (Hydrogen Index). International Journal of Coal Geology 78, 119-134.

Pohlman, J.W., Canuel, E.A., Chapman, N.R., Spence, G.D., Whiticar, M.J., Coffin, R.B., 2005. The origin of thermogenic gas hydrates on the northern Cascadia Margin as inferred from isotopic ($^{13}C/^{12}C$ and D/H) and molecular composition of hydrate and vent gas. Organic Geochemistry 33, 703–716.

Price, L.C., Schoell, M., 1995. Constraints on the origins of hydrocarbon gas from compositions of gases at their site of origin. Nature 378, 368–371.

Prinzhofer, A., Huc, A., 1995. Genetic and post-genetic molecular and isotopic fractionation in natural gas. Chemical Geology 126, 281–290.

Prinzhofer, A., Pernaton, E., 1997. Isotopically light methane in natural gas: bacterial imprint or diffusive fractionation? Chemical Geology 142, 193–200.

Qian, K., Zhao, Q., Wang, Z., 1996. The theory of coalbed methane exploration & development and experiment testing technique. Beijing: Petroleum Industry Press.

Rice, D.D., 1993. Composition and origins of coalbed gas. In: Hydrocarbons from Coal (Eds. B.E., Low and D.D., Rice), American Association of Petroleum Geologists, Tulsa, OK, 159–184.

Robinson, B.W., Hirner, A.V., Lyon, G.L., 1991. Stable carbon and sulfur isotope distributions of crude oil and source rock constituents from Burgan and Raudhatain oil fields (Kuwait), Chemical Geology 86, 295–306.

Sachse, D., Gleixner, G., Wilkes, H., Kahmen, A., 2010. Leaf wax *n*-alkane δD values of field-grown barely reflect leaf water δD values at the time of leaf formation. Geochimica et Coamochimica Acta 74, 6741–6750.

Saito, H., Suzuki, N., Takahashi, K.U., 2012. Simultaneous and sensitive analysis of inorganic and organic gaseous compounds by pulsed discharged helium ionization detector (PDHID). Geochemical journal 46, 255–259.

Sakata, S., Sano, Y., Maekawa, T., Igari, S., 1997. Hydrogen and carbon isotopic

composition of methane as evidence for biogenic origin of natural gases from the Green Tuff Basin, Japan. Organic Geochemistry 26, 399–407.

Schenk, H.J., DiPrimio, R., Horsfield, B., 1997. The conversion of oil into gas in petroleum reservoirs. Part 1: comparative kinetic investigation of gas generation from crude oils of lacustrine, marine and fluviodeltaic origin by programmed-temperature closed-system pyrolysis. Organic Geochemistry 26, 467–481.

Schimmelmann, A., Boudou, J.P., Lewan, M.D., Wintsch, R.P., 2001. Experimental controls on D/H and $^{13}C/^{12}C$ ratios of kerogen, bitumen and oil during hydrous pyrolysis. Organic Geochemistry 32, 1009–1018.

Schimmelmann, A., Lewan, M.D., Winsch, R.P., 1999. D/H istope ratios of kerogen, bitumen, oil, water in hydrous pyrolysis of source rocks containing kerogen types I, II, IIS, and III. Geochimica et Cosmochimica Acta 63, 3751–3766.

Schimmelmann, A., Sessions, A.L., Mastalerz, M., 2006. Hydrogen isotopic (D/H) composition of organic matter during diagenesis and thermal maturation. Annual Review of Earth and Planetary Sciences 34, 501–533.

Schoell, M., 1980. The hydrogen and carbon isotopic composition of methane from natural gases of various origins. Geochimica et Cosmochimica Acta 44, 649–661.

Schoell, M., 1988. Multiple origins of methane in the earth. Chemical Geology 71, 1–10.

Smith, J.W., Rigby, D., Gould, K.W., Hart, G., 1985. An isotopic study of hydrocarbon generation processes. Organic Geochemistry 8, 341–347.

Stahl, W.J., 1977. Carbon and nitrogen isotopes in hydrocarbon research andexploration. Chemical Geology 20, 121–149.

Strąpoć, D., Schimmelmann, A., Mastalerz, M., 2006. Carbon isotopic fractionation of CH_4 and CO_2 during canister desorption of coal. Organic Geochemistry 37, 152-164.

Suzuki, Y., Fujii, K., 1999. Evaluation of oil-generation potential on coals from Japan and

foreign countries. Bulletin of the Geological Survey of Japan 50, 407–422.

Takahashi, R., Aihara, A., 1989. Characteristic nature of sedimentation and coalification in the Tertiary system of the Japanese Islands. International Journal of Coal Geology 13, 437–453.

Takano, O., Waseda, A., 2003. Sequence stratigraphic architecture of a differentially subsiding bay to fluvial basin: the Eocene Ishikari Group, Ishicari Coal Field, Hokkaido, Japan. Sedimentary Geology 160, 131-158.

Tang, Y., Jenden, P.D., 1998. Modeling gas isotopic fractionation during thermogenic gas generation. ABS-PAP-ACS 215 (Part 1), 3–GEOC.

Tang, Y., Jenden, P.D., Nigrini, A., Teerman, S.C., 1996. Modeling early methane generation in coal. Energy & Fuels 10, 659–671.

Tang, Y., Perry, J.K., Jenden, P.D., Schoell, M., 2000. Mathematical modeling of stablecarbon isotope ratios in natural gases. Geochimica et Cosmochimica Acta 64, 2673–2687.

Tipple, B. J., Pagani, M., 2010. A 35 Myr North American leaf-wax compound-specific carbon and hydrogen isotope record: Implications for C_4 grasslands and hydrologic cycle dynamics. Earth and Planetary Science Letters 299, 250–262.

Waseda, A., Iwano, H., Takeda, N., 2002. Geochemical study on origin and maturity of natural gases. Journal of the Japanese Association for Petroleum Technology 67, 3–15.

Waseda, A., Nishita, H., 1998. Geochemical characteristics of terrigenous- and marine-sourced oils in Hokkaido, Japan. Organic Geochemistry 28, 27–41.

Whiticar, M.J., 1996. Stable isotope geochemistry of coals, humic kerogens and related natural gases. International Journal of coal geology 32, 191–215.

Wilkins, W.T.R., George, C.S., 2002. Coal as source rock for oil: a review. International Journal of Coal Geology 50, 317-361.

Yang, W., Liu, W., Leng, Q., Hren, M.T., Pagani, M., 2011. Variation in *n*-alkane δD values from terrestrial plants at high latitude: Implications for Paleoclimate reconstruction. Organic Geochemistry 42, 283–288.

Yessalina, S., Suzuki, N., Nishita, H., Waseda, A., 2006. Higher plant biomarkers in Paleogene crude oils from the Yufutsu oil- and gasfield and offshore wildcats, Japan. Journal of Petroleum Geology 29, 327–336.

Zhang, T., Krooss, B.M., 2001. Experimental investigation on the carbon isotope fractionation of methane during gas migration by diffusion through sedimentary rocks at elevated temperature and pressure. Geochimica et Cosmochimica Acta 65, 2723–2742.

[Table Captions]

Table 1. Elemental composition and vitrinite reflectance of the original Eocene Yubari subbituminous coal used for the pyrolysis experiments.

Table 2. Results of the anhydrous pyrolysis experiment for Eocene Yubari coal.

[Figure Captions]

Fig. 1 Typical PDHID chromatograms of (a) expelled gas, (b) desorbed gas, (c) residual free gas, and (d) residual adsorbed gas from artificially matured Eocene subbituminous coal pyrolyzed at 370°C for 72 h. VR_r was measured as 1.47%.

Fig. 2 Changes in the gas compositions of the expelled, desorbed, residual free, and residual adsorbed gases with increasing maturity. $CH_4/(C_2H_6+C_3H_8)$ vs. $VR_r(\%)$ for the expelled and desorbed gases (a) and for the residual free and adsorbed gases (b). $CO_2/(CO_2+CH_4)$ vs. $VR_r(\%)$ for the expelled and desorbed gases (c) and for the residual free and adsorbed gases (d). The residual free and adsorbed gas compositions of the original Eocene Yubari subbituminous coal are also shown in (b) and (d).

Fig. 3 Changes in $\delta^{13}C$ values of C_1–C_3 and CO_2 in the expelled, desorbed, and residual free gases with increasing maturity.

Fig. 4 Changes in $\delta^{2}H$ values of C_1–C_3 in the expelled, desorbed, and residual free gases with increasing maturity.

Fig. 5 Comparison among the evolution paths of (a) $\delta^{13}C_1$ vs. $\delta^{13}C_2$ values and (b) $\delta^{13}C_2$ vs. $\delta^{13}C_3$ values of gases from Type II kerogen, Type III kerogen, and Eocene Yubari subbituminous coal. The evolution paths of $\delta^{13}C$ values of gases from Type II and Type III kerogens were calculated based on the geochemical model of Berner and Faber (1996) using the original $\delta^{13}C$ values of Type II and Type III kerogens

proposed by Waseda and Nishita (1998) and Waseda et al. (2002). The differential $\delta^{13}C$ values of gases were calculated based on the cumulative changes in the $\delta^{13}C$ values and the volumes of C_1, C_2, and C_3 generated by the closed-system pyrolysis.

Fig. 6. Changes in the differential $\delta^{2}H$ value of C_1 with increasing maturation during pyrolysis of Eocene Yubari subbituminous coal. The differential $\delta^{2}H$ value of C_1 was calculated based on the cumulative changes in the $\delta^{2}H$ value and the volume of C_1 generated by the closed-system pyrolysis. The changes in the $\delta^{2}H$ values of C_1 from Type II and Type III kerogens with VR_r are from Berner et al. (1995).

Table 1

VR_r (%)	C (wt%)	H (wt%)	O (wt%)	N (wt%)	S (wt%)	Atomic H/C	Atomic O/C
0.46	77.8	6.31	14.5	1.28	0.14	0.97	0.14

(dry ash free)

Table 2

Sample code	Temp. (ºC)	Time (hrs)	VR_r (%)	Gas Fraction	Yields of gas (μL/g coal)										$\frac{C_1}{C_2+C_3}$	$\frac{CO_2}{CO_2+C_1}$	$\delta^{13}C$ (‰)				$\delta^{2}H$ (‰)		
					H_2	CO	C_1	CO_2	C_2H_4	C_2	C_3H_6	C_3	*i*-C_4	*n*-C_4			C_1	C_2	C_3	CO_2	C_1	C_2	C_3
Original coal			0.46	Residual (f)	n.d.	25.0	10.7	54.0	1.5	2.5	tr.	0.5	tr.	tr.	3.55	0.83	-30.8	n.d.	n.d.	-24.0	-217	n.d.	n.d.
				Residual (a)	1.9	8.3	0.5	87.3	0.1	0.4	tr.	0.9	0.1	0.3	0.39	0.99	n.d.	n.d.	n.d.	n.d.	n.d.	n.d.	n.d.
AMC #1	325	24	0.53	Expelled	190.6	817.0	713.4	878.4	11.3	188.8	44.0	192.2	39.6	52.4	1.87	0.55	-34.8	-29.5	-26.8	-24.9	-337	-267	-278
				Desorbed	tr.	2.8	28.4	47.1	0.3	8.1	1.0	6.9	0.9	2.7	1.89	0.62	-40.0	-32.6	-28.2	-27.4	-328	-284	-283
				Residual (f)	28.8	3.2	9.6	13.0	1.1	10.0	0.5	7.3	0.4	0.6	0.56	0.58	-28.3	-29.7	-27.6	-22.7	-199	n.d.	n.d.
				Residual (a)	0.5	2.1	0.3	26.5	tr.	0.3	tr.	5.7	2.7	5.2	0.06	0.99	n.d.	n.d.	n.d.	n.d.	n.d.	n.d.	n.d.
AMC #2	330	72	0.60	Expelled	410.8	739.2	1395	876.8	13.3	409.9	43.1	389.1	99.3	135.1	1.75	0.39	-35.8	-29.8	-26.4	-24.5	-325	-266	-233
				Desorbed	5.8	4.8	53.9	45.9	0.3	16.5	1.1	18.0	3.0	8.9	1.56	0.46	-41.5	-32.4	-28.0	-26.0	-330	-262	-238
				Residual (f)	n.d.	n.d.	n.d.	n.d.	n.d.	n.d.	n.d.	n.d.	n.d.	n.d.	n.d.	n.d.	n.d.	n.d.	n.d.	n.d.	n.d.	n.d.	n.d.
				Residual (a)	tr.	0.5	0.2	37.1	tr.	0.4	tr.	7.0	5.2	10.6	0.03	0.99	n.d.	n.d.	n.d.	n.d.	n.d.	n.d.	n.d.
AMC #3	350	48	1.03	Expelled	1011.5	1269.4	2631.2	1571.8	25.4	961.5	84.5	890.2	249.6	436.2	1.42	0.37	-36.7	-29.4	-26.6	-23.3	-325	-282	-275
				Desorbed	tr.	8.7	127.6	60.0	1.0	75.8	3.4	63.2	9.7	33.2	0.92	0.32	-29.8	-29.0	-26.9	-24.5	-315	-275	-254
				Residual (f)	n.d.	tr.	14.7	12.7	0.6	37.5	2.3	54.4	7.7	19.6	0.16	0.46	-28.3	-28.7	-27.2	-25.9	-199	-265	-247
				Residual (a)	0.3	4.4	0.3	42.6	tr.	0.5	tr.	17.8	14.2	48.1	0.02	0.99	n.d.	n.d.	n.d.	n.d.	n.d.	n.d.	n.d.
AMC #4	350	72	1.29	Expelled	1279.3	1040.4	3033.3	1123.1	25.8	1059.6	92.1	1020.3	269.6	530.9	1.46	0.27	-38.1	-29.7	-26.5	-24.5	-313	-261	-241
				Desorbed	tr.	1.4	96.2	27.7	0.7	74.9	2.8	58.3	6.4	30.4	0.72	0.22	-33.0	-29.7	-27.2	-21.1	-309	-270	-250
				Residual (f)	n.d.	tr.	14.0	10.3	0.4	30.8	1.6	43.1	5.8	14.8	0.19	0.42	-28.5	-28.8	-26.8	-20.5	-183	-260	-236
				Residual (a)	0.3	2.4	0.2	30.8	tr.	0.4	tr.	15.5	13.4	44.2	0.01	0.99	n.d.	n.d.	n.d.	n.d.	n.d.	n.d.	n.d.
AMC #5	370	72	1.46	Expelled	2409.3	1366.8	5383.5	1849.4	42.7	1925.3	135.2	1592.6	421.0	925.6	1.53	0.26	-37.9	-29.0	-26.7	-23.9	-297	-254	-230
				Desorbed	tr.	7.3	306.4	115.9	1.6	116.1	2.2	37.0	1.0	10.7	2.00	0.27	-38.5	-30.2	-28.4	-25.2	-312	-269	-242
				Residual (f)	184.5	13.7	62.8	7.6	1.5	80.8	0.8	35.8	1.0	3.3	0.54	0.11	-29.8	-29.7	-26.7	-23.9	-195	-253	-222
				Residual (a)	1.2	4.7	0.6	58.6	tr.	5.1	tr.	81.8	16.0	72.3	0.01	0.99	n.d.	n.d.	n.d.	n.d.	n.d.	n.d.	n.d.
AMC #6	390	72	1.70	Expelled	3102.8	1522.9	8798.0	2529.6	57.0	3055.1	178.8	2336.7	581.1	1340.8	1.63	0.22	-35.9	-28.3	-26.6	-22.4	-291	-245	-222
				Desorbed	tr.	0.5	372.7	145.0	1.2	95.2	1.1	24.9	0.7	7.5	3.10	0.28	-38.8	-31.3	-29.7	-23.1	-309	-253	n.d.
				Residual (f)	245.3	9.7	105.5	65.9	1.4	153.7	0.9	55.9	1.7	5.6	0.50	0.38	-29.1	-29.2	-27.0	-22.2	-220	-255	-207
				Residual (a)	1.4	4.7	0.6	59.2	tr.	5.1	tr.	81.8	16.1	72.8	0.01	0.99	n.d.	n.d.	n.d.	n.d.	n.d.	n.d.	n.d.
AMC #7	390	168	1.80	Expelled	2771.6	1646.6	11677.0	2802.4	70.5	3574.8	225.5	2854.5	788.6	1778.6	1.82	0.19	-34.3	-27.6	-25.5	-22.7	-257	-229	-205
				Desorbed	tr.	7.1	374.8	136.5	0.9	77.2	0.4	10.4	0.1	1.9	4.28	0.27	-36.8	-30.6	n.d.	-24.3	-280	-247	n.d.
				Residual (f)	179.7	28.4	125.0	64.2	0.7	106.6	0.1	10.6	0.0	0.2	1.07	0.34	-32.8	-29.2	-26.1	-24.4	-239	-231	n.d.
				Residual (a)	1.9	10.6	1.1	116.5	tr.	13.8	tr.	111.2	5.7	26.1	0.01	0.99	n.d.	n.d.	n.d.	n.d.	n.d.	n.d.	n.d.

n.d.: not determined, tr.:trace, Residual (f): residual free gas, Residual (a): residual adsorbed gas

Fig. 1

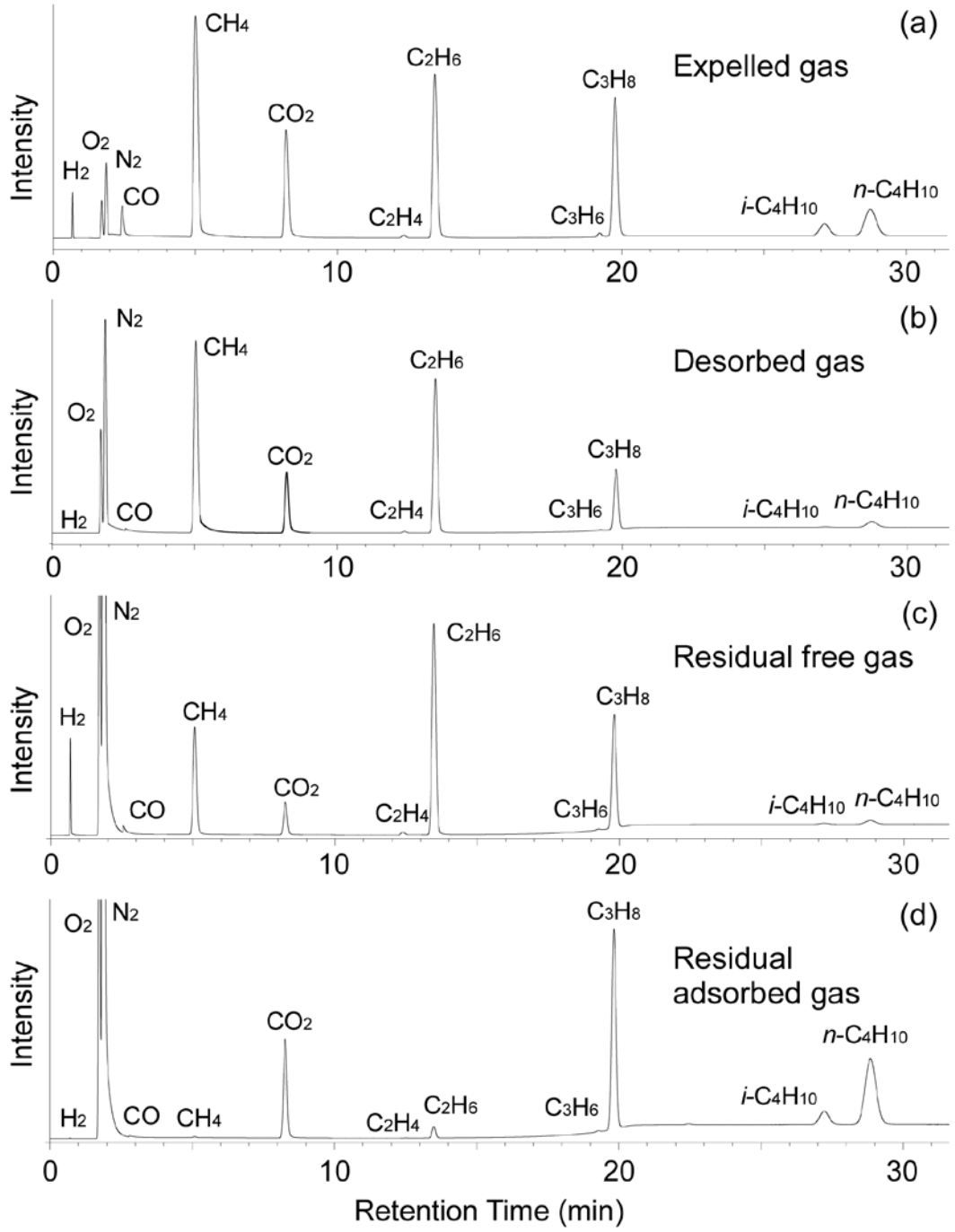
(a)
Expelled gas
(b)
Desorbed gas
(c)
Residual free gas
(d)
Residual adsorbed gas
Intensity
H2
O2
N2
CO
CH4
CO2
C2H4
C2H6
C3H6
C3H8
i-C4H10
n-C4H10
0
10
20
30
Retention Time (min)

Fig. 2

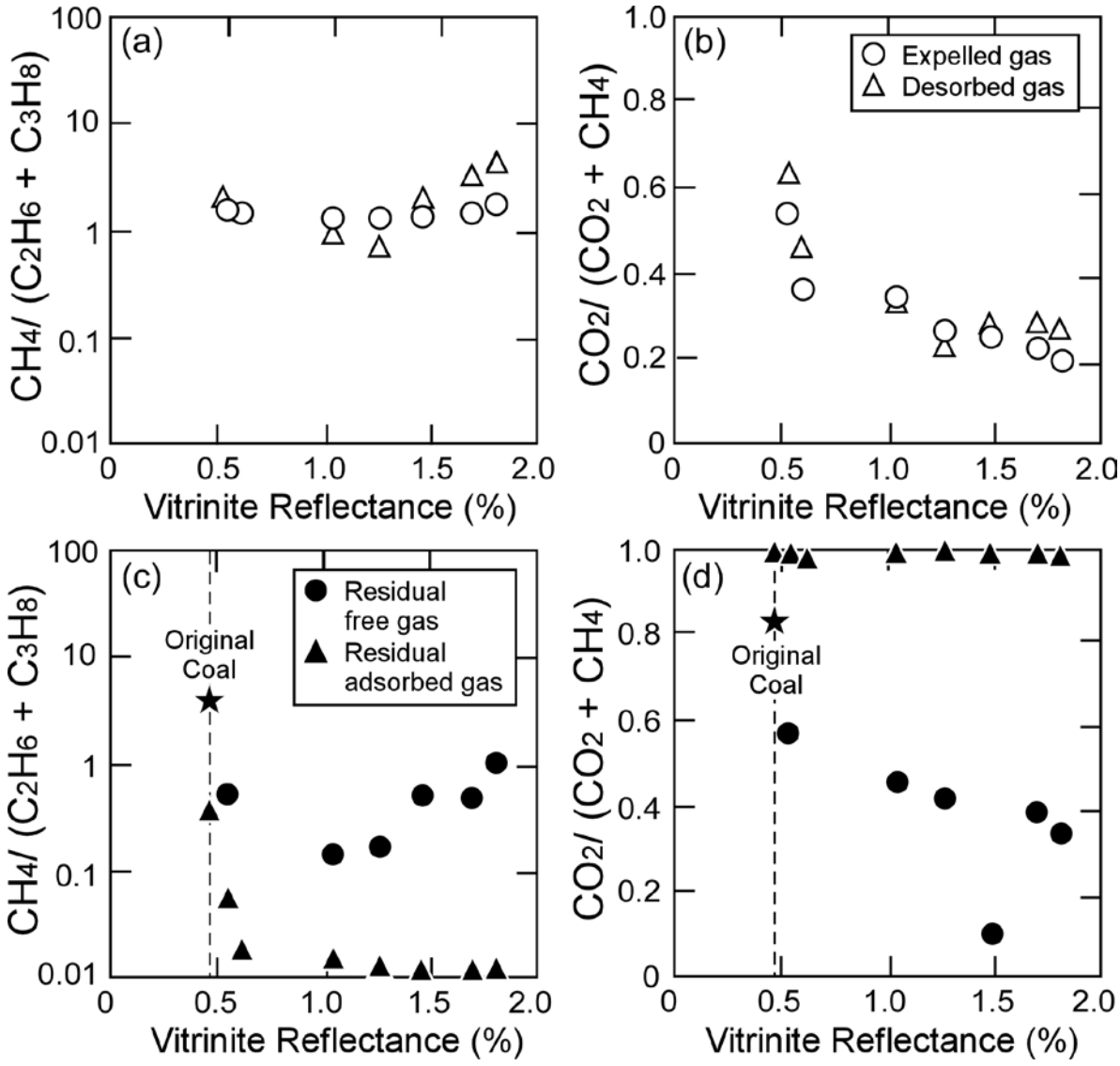
(a)
CH4/ (C2H6 + C3H8)
100
10
1
0.1
0.01
0
0.5
1.0
1.5
2.0
Vitrinite Reflectance (%)
(b)
Expelled gas
Desorbed gas
CO2/ (CO2 + CH4)
1.0
0.8
0.6
0.4
0.2
0
Vitrinite Reflectance (%)
(c)
Residual free gas
Residual adsorbed gas
Original Coal
CH4/ (C2H6 + C3H8)
Vitrinite Reflectance (%)
(d)
Original Coal
CO2/ (CO2 + CH4)
Vitrinite Reflectance (%)

Fig. 3

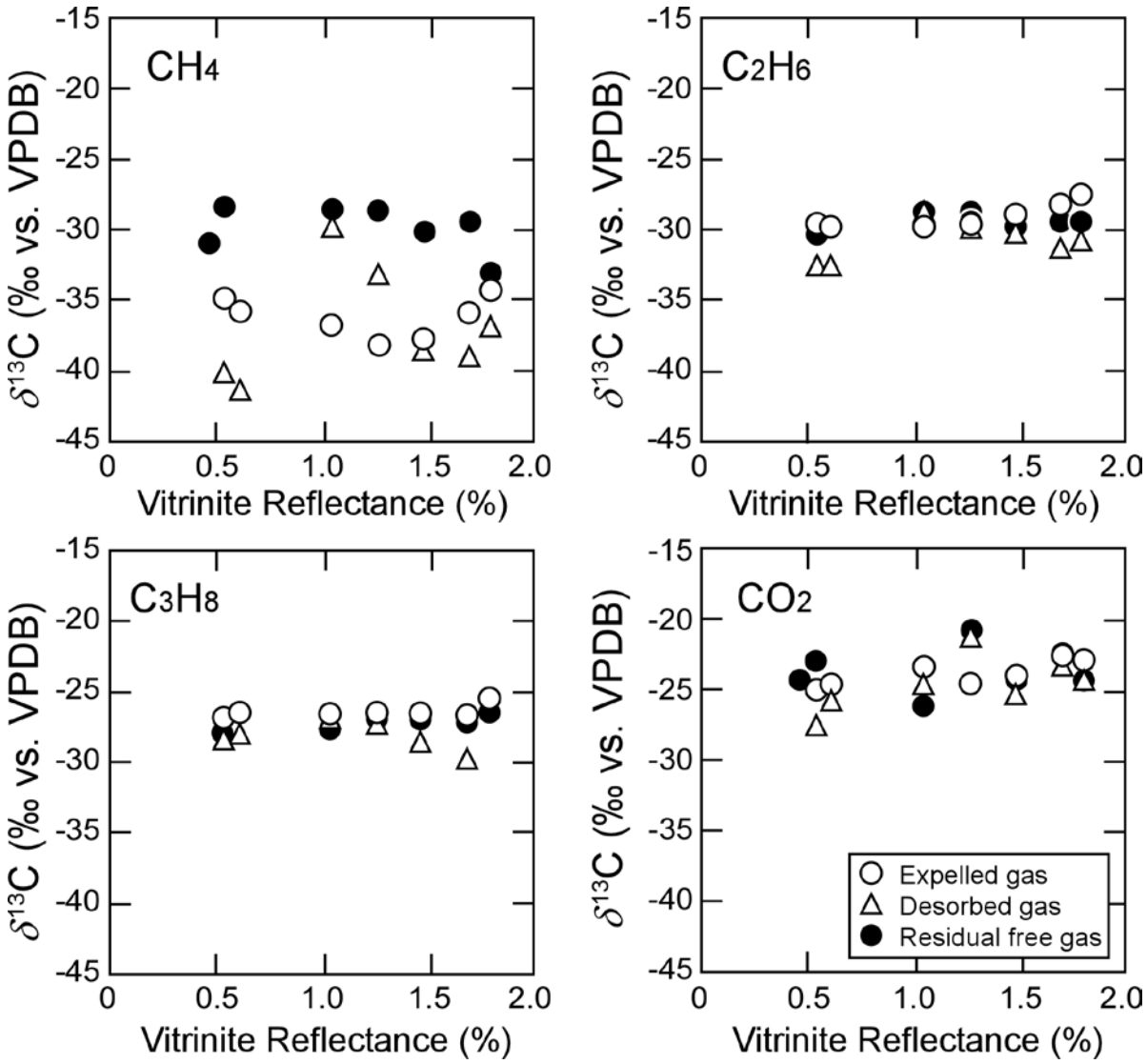
CH4
C2H6
C3H8
CO2
δ13C (‰ vs. VPDB)
Vitrinite Reflectance (%)
-15
-20
-25
-30
-35
-40
-45
0
0.5
1.0
1.5
2.0
Expelled gas
Desorbed gas
Residual free gas

Fig. 4

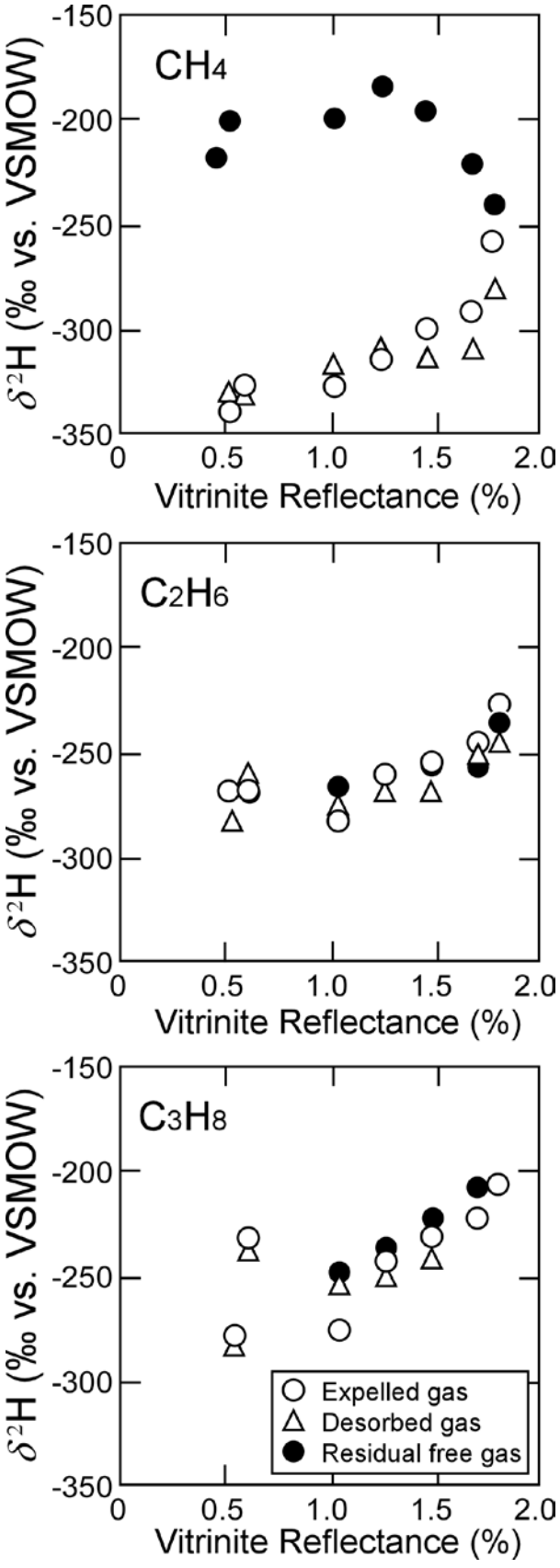
CH4
C2H6
C3H8
δ2H (‰ vs. VSMOW)
-150
-200
-250
-300
-350
0
0.5
1.0
1.5
2.0
Vitrinite Reflectance (%)
Expelled gas
Desorbed gas
Residual free gas

Fig. 5

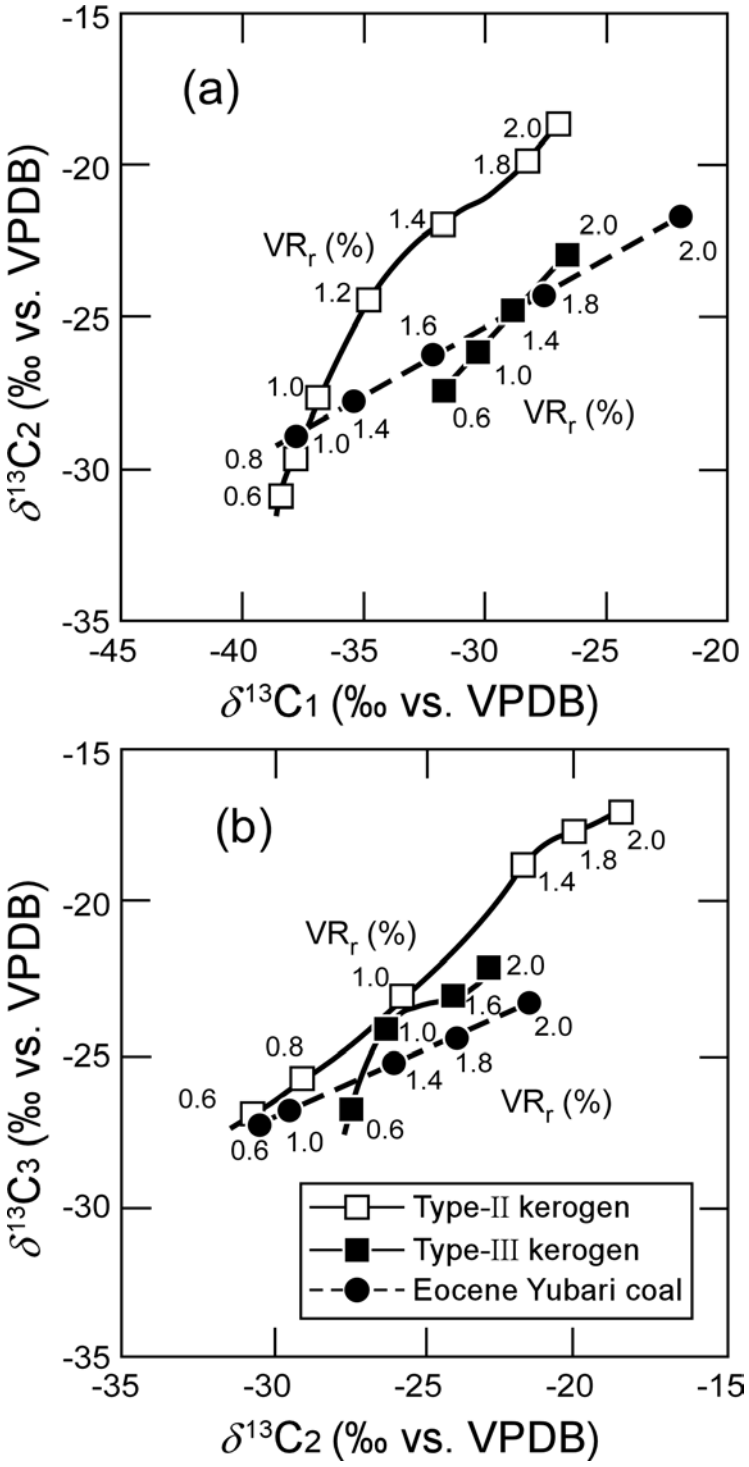
(a)
$\delta^{13}C_2$ (‰ vs. VPDB)
$\delta^{13}C_1$ (‰ vs. VPDB)
VR$_r$ (%)
VR$_r$ (%)
(b)
$\delta^{13}C_3$ (‰ vs. VPDB)
$\delta^{13}C_2$ (‰ vs. VPDB)
VR$_r$ (%)
VR$_r$ (%)
Type-II kerogen
Type-III kerogen
Eocene Yubari coal

Fig. 6

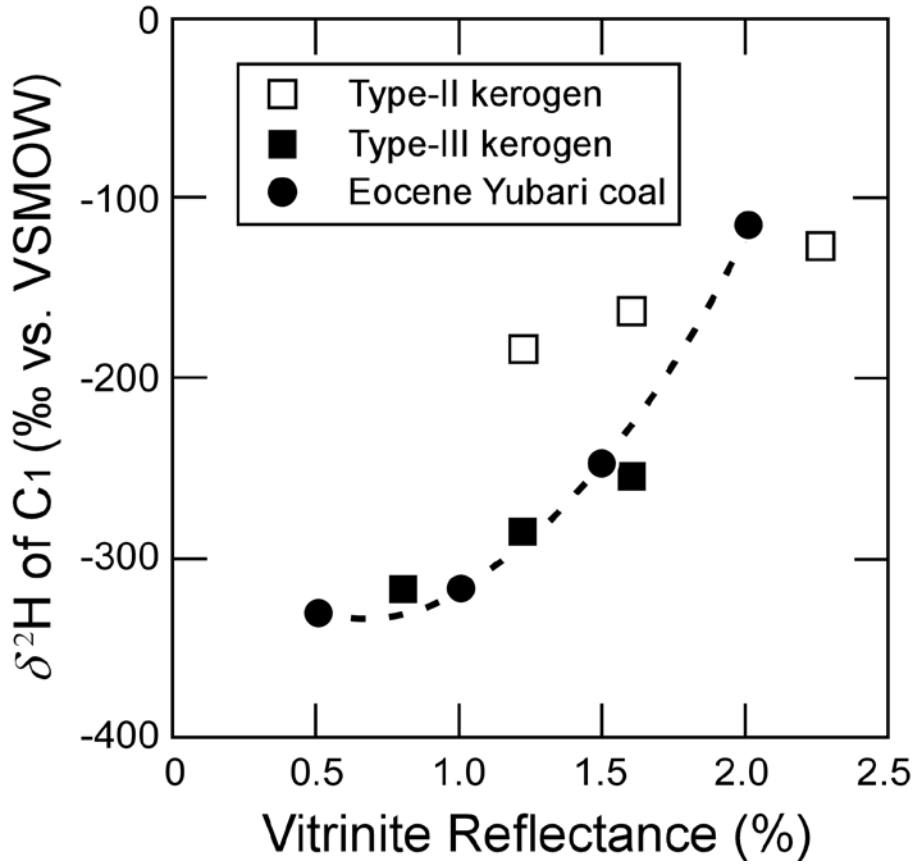
Type-II kerogen
Type-III kerogen
Eocene Yubari coal
δ²H of C₁ (‰ vs. VSMOW)
0
-100
-200
-300
-400
0
0.5
1.0
1.5
2.0
2.5
Vitrinite Reflectance (%)